Spatial Control of Condensation and Freezing on Superhydrophobic Surfaces with Hydrophilic Patches

*Lidiya Mishchenko, Mughees Khan, Joanna Aizenberg, and Benjamin D. Hatton**

Certain natural organisms use micro-patterned surface chemistry, or ice-nucleating species, to control water condensation and ice nucleation for survival under extreme conditions. As an analogy to these biological approaches, it is shown that functionalized, hydrophilic polymers and particles deposited on the tips of superhydrophobic posts induce precise topographical control over water condensation and freezing at the micrometer scale. A bottom-up deposition process is used to take advantage of the limited contact area of a non-wetting aqueous solution on a superhydrophobic surface. Hydrophilic polymer deposition on the tips of these geometrical structures allows spatial control over the nucleation, growth, and coalescence of micrometer-scale water droplets. The hydrophilic tips nucleate water droplets with extremely uniform nucleation and growth rates, uniform sizes, an increased stability against coalescence, and asymmetric droplet morphologies. Control of freezing behavior is also demonstrated via deposition of ice-nucleating AgI nanoparticles on the tips of these structures. This combination of the hydrophilic polymer and AgI particles on the tips was used to achieve templating of ice nucleation at the micrometer scale. Preliminary results indicate that control over ice crystal size, spatial symmetry, and position might be possible with this method. This type of approach can serve as a platform for systematically analyzing micrometer-scale condensation and freezing phenomena, and as a model for natural systems.

1. Introduction

Certain plants and insects have evolved micro-patterned hydrophilic/hydrophobic surface chemistries and topographies to control the condensation of water. The Namib dessert beetle uses its bumpy back with hydrophilic and hydrophobic patches to selectively condense and channel water droplets from humid air towards its mouth.[1] Recently, Ju et al. demonstrated a directional wetting that a cactus species (*Opuntia microdasys*) uses on its spines for fog collection.[2] Also, certain types of water ferns are able to withstand turbulent periods of water submersion without wetting by using a small number of distributed hydrophilic patches on their leaves.[3] Bacteria[4] and fungal spores[5] have been shown to control ice nucleation on plant leaf surfaces (to induce damage, in the case of *Pseudomonas syringae*), or induce cloud seeding in the atmosphere. Finally, many fish, amphibious and insect species use ice-nucleating agents in solution to control ice nucleation and growth to survive extreme conditions. Various insects, such as the goldenrod gall fly, survive cold weather conditions using ice-nucleating proteins to reduce the freezing temperature and allow their larvae to controllably freeze without causing cell damage.[6] Herein, as an analogy to these biological approaches, topographical control over water condensation and freezing is achieved at the micrometer scale via the deposition of hydrophilic polymers and particles on the tips of selected patterned, superhydrophobic surfaces (SHS).

Spatial control of condensation has been explored in the literature from different perspectives. Two-dimensional (2D) control of water condensation on surfaces was achieved using patterned self-assembled monolayers of alkanethiolates.[7] Condensation on structured superhydrophobic surfaces with uniform surface chemistry has also been studied,[8–11] primarily focusing on droplet mobility. Milijkovic et al. showed that condensation on nanoscale superhydrophobic surfaces can improve heat transfer efficiently through droplet dewetting (jumping).[12] Varanasi et al. have shown that condensation can be spatially controlled on superhydrophobic surfaces via a top-down lithography technique.[13] Though establishing that water condensation can in fact be controlled on topographic surfaces using patterned hydrophilic regions, the experimental complexity of the surface patterning approach and the lack of systematic testing in the latter work leaves many aspects of condensation on SHS unexplored. Moreover, to the best of our knowledge, topographical control of highly localized ice nucleation at the micrometer scale has not been addressed either in the previous work or in the literature in general. The objective of this work is to use a bottom-up fabrication approach to achieve a spatial control over the nucleation, growth, and coalescence of water droplets, and their freezing, at the micrometer length scale. Herein we demonstrate a novel approach

L. Mishchenko, Dr. M. Khan, Prof. J. Aizenberg, Prof. B. D. Hatton
Wyss Institute for Bio-inspired Engineering
School of Engineering and Applied Sciences
Harvard University
Cambridge, MA 02138, USA
E-mail: benjamin.hatton@utoronto.ca
Prof. B. D. Hatton
Department of Materials Science and Engineering
University of Toronto
Toronto, ON, Canada

DOI: 10.1002/adfm.201300418

for highly localized ice nucleation by using ice-nucleating particles positioned at the tips of the superhydrophobic posts. This new method opens a new platform for systematically analyzing condensation and freezing phenomena with a wide range of topographically-patterned geometries. Water and ice nucleation in nature are still not very well understood, and such an experimental platform may be useful in testing the conditions and mechanisms associated with many natural systems (i.e., cloud seeding, ice nucleating proteins, etc.).

2. Results and Discussion

A bottom-up approach to locally deposit materials from solution onto the tops of structured superhydrophobic surfaces has recently been demonstrated.[14,15] This approach is possible because of the limited contact area of these surfaces with an aqueous droplet (**Figure 1**A). In particular, the ability of polyvinyl alcohol (PVA) to adsorb onto most hydrophobic surfaces from solution[16] allows a simple bottom-up approach[15] to creating localized hydrophilic tips on superhydrophobic surfaces (Figure 1B). Volmer's classical nucleation theory[13,17] and experimental nucleation studies[18] predict that the nucleation rate of water on hydrophilic surfaces will be significantly higher than on the hydrophobic surfaces. Accordingly, localized hydrophilic PVA-coated tips are expected to preferentially nucleate water upon cooling of a surface below the dew point (Figure 1C). Thus, water nucleation can be spatially controlled by taking advantage of various microscopic SHS geometries that can be patterned in silicon (Figure 1 inset, see Experimental Section for materials synthesis).

The spatial control of nucleation with PVA tips is first demonstrated with a 'blade' geometry. Without hydrophilic tip functionalization, the blade surface is homogeneously hydrophobic. Thus, this surface has no preferred site for water nucleation and microscopic water droplets randomly nucleate both on the tips and the sides of the 3D structures. This random nucleation leads to the coalescence of large wetting droplets throughout the structure, as observed from the top with an optical microscope (**Figure 2**A, Supporting Information Figure S1), and at an angle with an environmental SEM (Figure 2B). However, with PVA selectively deposited on the tips of the blade structure, nucleation of water droplets becomes highly uniform, and is localized only at the tips of the blades (Figure 2B,C). In fact, even as the

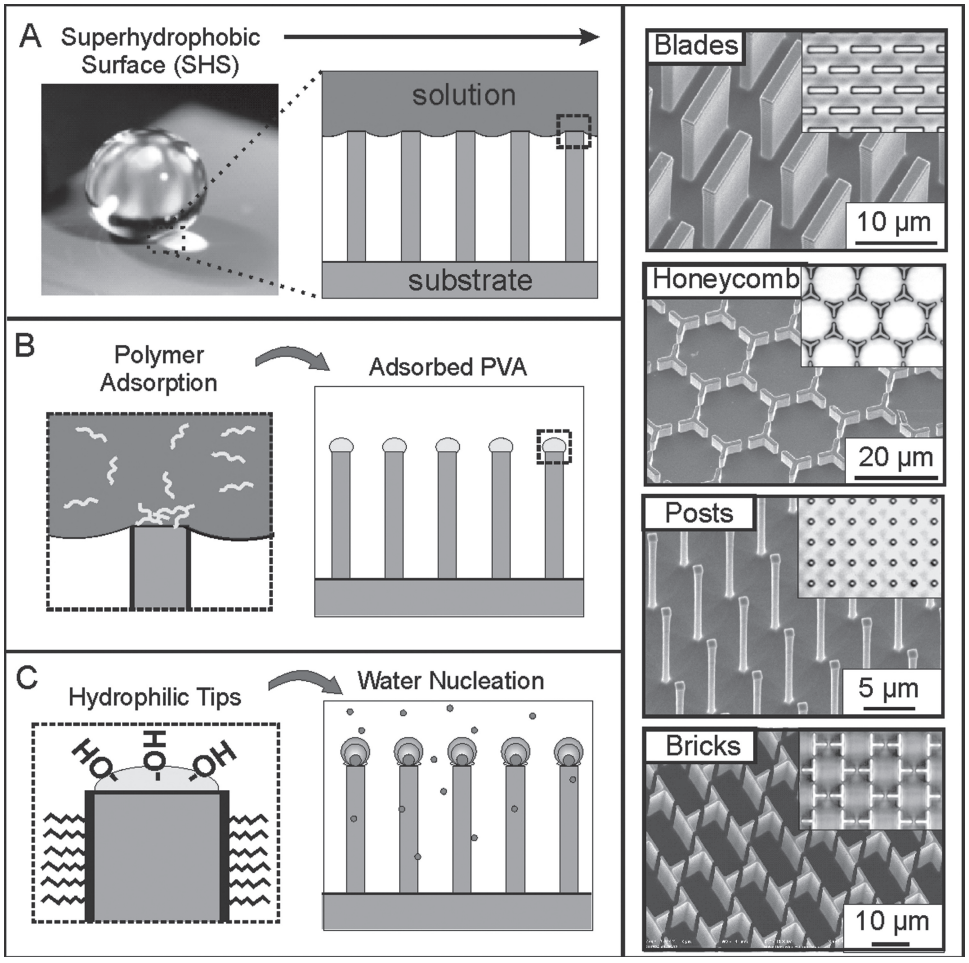

Figure 1. Tip deposition on superhydrophobic surfaces (SHS). A) The limited area of contact of an aqueous solution with a SHS is shown. Right: SEM and optical (insets) images of various geometries of SHS. B) An aqueous polymer (polyvinyl alcohol) adsorbs to the tips of an SHS. C) PVA adsorption renders the tips hydrophilic, resulting in localized water nucleation upon cooling of the surface below the dew point.

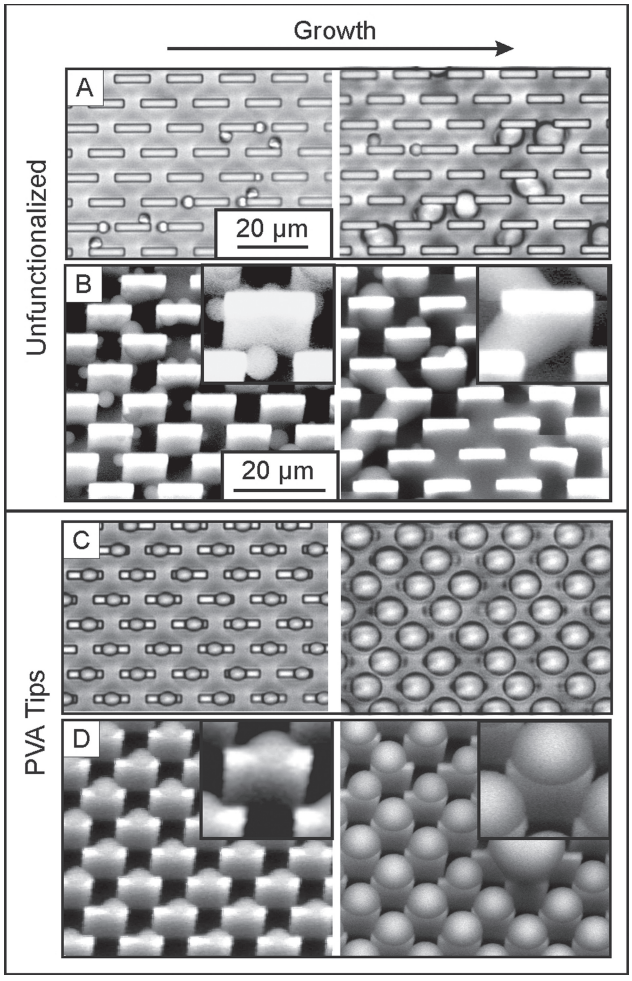

Figure 2. Optical (A,C) and environmental scanning electron microscope (B,D) images of water condensation on blade SHS. On uniformly hydrophobic blade surfaces, water nucleation is random, resulting in wetting films (A,B). With PVA-coated blades, water nucleation is limited only to the hydrophilic tips (C,D). The nucleation of the droplets is highly homogeneous, resulting in simultaneous and uniform growth of all the droplets.

droplets grow and coalesce, they remain on the tips of the structure (Supporting Information, video 1). This is an effect never before observed in the literature, and has interesting consequences for efficient water collection due to the droplet mobility.

This spatial control of condensation can be extended to other topographic geometries. The simplest geometry is that of posts. As with the blades, random nucleation and coalescence normally occurs around hydrophobic posts (**Figure 3**A). However, with PVA tips, microscopic water droplets nucleate simultaneously on the top of each post, and grow at a uniform rate, changing the apparent diameter of the posts (Figure 3B). This uniformity of growth, combined with different possible symmetries of post arrays (i.e., hexagonal, square), allow us to control the sequence of Ostwald ripening events that occur between the droplets as they grow beyond a certain critical size (Supporting Information Figure S2). Other topographic geometries, such as honeycomb (Figure 3C) and brick (Figure 3D), allow us to tailor the localized nucleation of water to achieve different patterns of uniform droplets. In the brick and honeycomb geometries without PVA tips, it appears as though droplets prefer to nucleate at locations that maximize their contact with the silicon surface, at corners and edges next to the bottom of the pattern. This behavior is well known in classical nucleation theory.[19] It is thus interesting that the hydrophilic tips from PVA adsorption force the system to be dominated by nucleation at the tips rather than corners. The nucleation of water on triangular or rectangular tips also forces the droplets to take on asymmetrical shapes (Figure 3C,D(ii)), which are at a higher energy state than that of a purely spherical droplet (which minimizes its surface to volume ratio).

The size of the geometric feature also plays a role in controlling water nucleation and coalescence. By coating the tips of blades of different lengths with PVA, we are able to change the number and size of droplets that grow on each individual blade (**Figure 4**). With small blades, only one droplet nucleates and grows in the middle of each blade (Figure 4A). With longer blades, a uniform array of two droplets ("dumbbells") per blade emerges (Figure 4B). With the longest blades, smaller droplets nucleate and coalesce to form large single droplets positioned randomly along the blades. With the large blades, one can observe an effect not easily seen with the smaller blades (Supporting Information, video 2) where the PVA tips initially nucleate a thin film of water, changing the color of the tips. The thin film nucleation is followed by the emergence of droplets. This result is consistent with film rupture theory that claims water vapor first condenses on cold surfaces and forms a micro-scale thin liquid film, only breaking up into droplets after reaching a critical thickness.[20] One interesting feature of note in this experiment is how close the water droplets come to touching each other before coalescing. One possible reason for this is that some of the PVA on the tips of the blades coats the nucleating droplet, and delays coalescence. Because PVA is a known amphiphilic stabilizer[21] that readily adsorbs to the water—air interface,[22] it is possible that it helps keep the droplets from coalescing either by lowering their surface energy as a surfactant or by creating a repulsive force between adjacent droplets. An analogous study observed that mercury droplets can be stabilized from coalescence by allowing self-assembled monolayers of alkane thiols to form on their surface.[23]

Since this work investigates a templating approach to controlling different physical states of water, ice nucleation naturally emerges as another point of interest. The unique bottom-up approach to depositing PVA onto surfaces can be extended to other water-soluble polymers and even aqueous suspensions of nanoparticles.[15] Thus, we can begin to investigate the effect of silver iodide (AgI) nanoparticles as ice-nucleators[24–26] on the tips of SHS. It has been shown that the surface charge of silver iodide can be controlled by changing the concentration of I^- and Ag^+ ions in solution.[27] We observed, along with other previous papers, that AgI sols synthesized and suspended under higher concentrations of Ag^+ are less stable and reproducible than AgI sols in neutral or I^--rich conditions.[28] We also noticed that nanoparticles from Ag^+-rich sols are less consistent in ice nucleation behavior. For these reasons, we use AgI particles derived from I^--rich sols in our experiments, rendering them negatively charged under neutral conditions. As

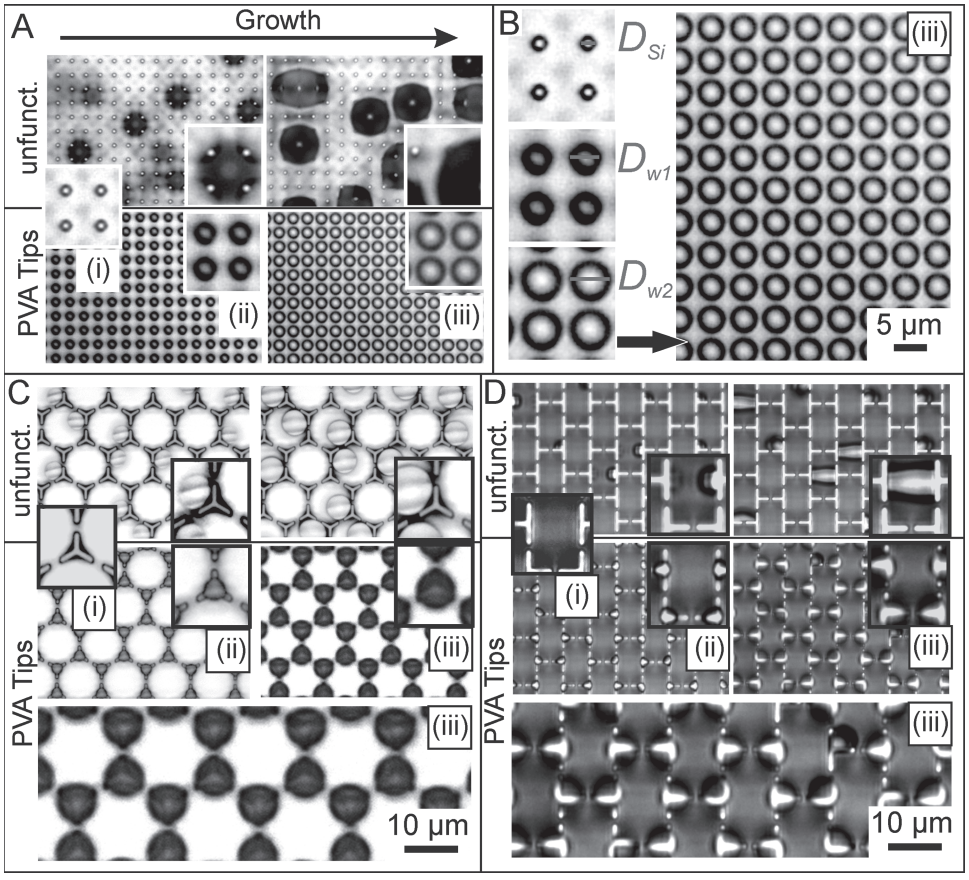

Figure 3. Optical images of the nucleation and growth of water condensation on various superhydrophobic surface geometries. A) Condensation on hydrophobic posts is random, resulting in wetting films. B) Condensation on posts with PVA tips (i–iii) is uniform, increasing the apparent diameter of the posts from the initial silicon post diameter (D_{Si}) to larger diameters of the water droplets (D_{w1}-D_{w2}). Condensation on C) honeycomb and D) brick SHS follows a similar pattern to the posts. On unfunctionalized (hydrophobic) patterns, droplets condense randomly, preferring corners and edges near the bottom of the substrate. With PVA tips, droplets uniformly condense on the tops of the structures. Due to the geometry of the tips, droplets condense into asymmetrical shapes (insets (ii)).

a preliminary experiment, poly-L-lysine, another water-soluble polymer, is used to attach AgI nanoparticles to a post array (**Figure 5**A). Because poly-L-lysine is positively charged under neutral conditions due to protonated amine groups, and AgI is negatively charged, AgI nanoparticles are electrostatically attracted to the adsorbed poly-L-lysine on the tops of the posts (Figure 5B). Macroscopic water droplets, deposited onto post surfaces with either uncoated (hydrophobic) tips, or tips coated with poly-L-lysine and AgI, are used to test the activity of the nanoparticles. Droplets deposited on AgI tips consistently were found to freeze at −5 °C, while droplets on the control sample do not freeze at this temperature for at least 5 min (Figure 5C). Droplets are also able to retain their discrete morphologies after freezing, which indicates that the freezing event does not induce Wenzel wetting into the structure (note: poly-L-lysine alone on tips has no effect on the freezing behavior of drops).

We can now combine the reproducible water and ice nucleation behavior observed in the two previous systems by using both PVA and AgI on the tips. Because both materials are negatively charged in aqueous solution, we first deposit PVA, which spontaneously physically adsorbs on the tips of a blade sample,[15] then attach positively-charged colloids (amidine-functionalized PS particles) onto those tips from solution, and finally attach AgI particles onto the amidine-functionalized colloids (**Figure 6**A,B). With both PVA and AgI on the tips of two different blade geometries, we are able to uniformly condense water droplets on all the tips and observe how these microscopic droplets behave as ice nucleation begins, forcing ice crystals to only form at the tips of the structures (Supporting Information, video 3). The results indicate that the spacing and symmetry of the geometrical blade arrays affect the structure of the ice crystals, making them significantly deviate from their normal hexagonal shape. With the staggered blade system, the ice crystals form square-shaped ice crystals with diagonal symmetry (Figure 6C). There is also roughly one ice crystal per blade, which corresponds to the number of water droplets per blade before freezing occurred. With longer, aligned blades, many of the ice crystals are still square (or rhomboidal), but are aligned linearly with the blades (Figure 6B). The size of the crystals is also approximately half of the blade length (approximately 5–10 μm), corresponding again to the number of droplets that coalesced on the blades before freezing. Certain blades

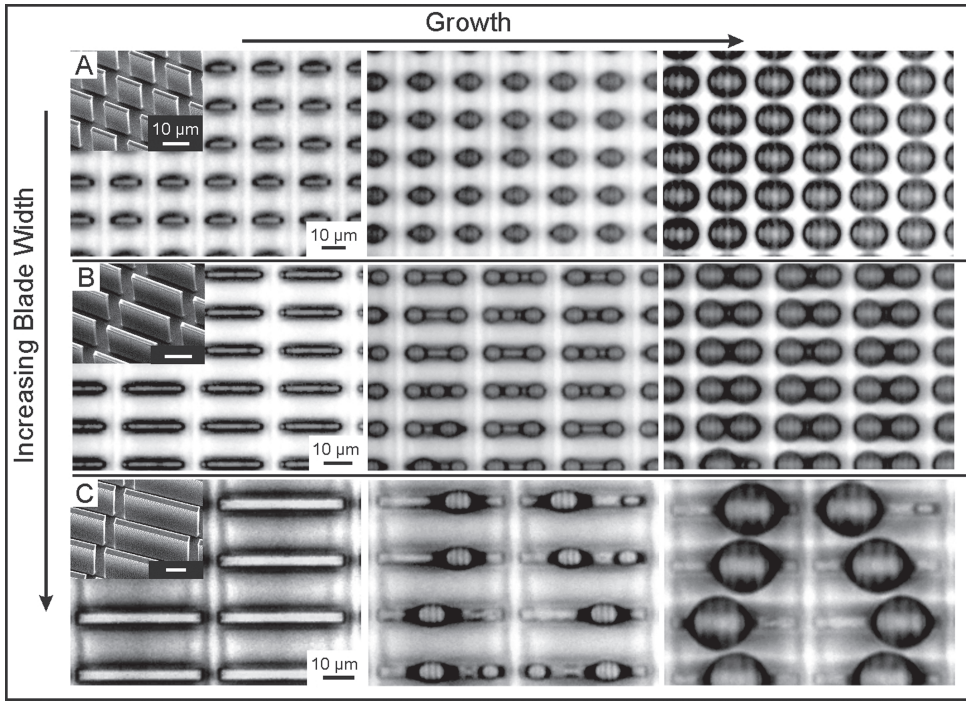

Figure 4. Geometrical control of droplet coalescence. PVA tip functionalization of three different blade geometries results in different droplet condensation patterns. A) The use of small blades results in the uniform condensation of one centered droplet per blade. B) Blades of intermediate length lead to two droplets per blade in a "dumbbell shape." C) The longest blades nucleate a thin film of water, which breaks up into droplets that coalesce to form large, randomly positioned single droplets.

produced doublet ice crystals (Figure 6D) of ≈20 μm, leaving some blades without crystals. These condensation (Supporting Information Figure S2) and freezing (Figure 6D) coalescence behaviors are intriguing and would benefit from a more detailed theoretical model.

It is noteworthy that in the ice nucleation system, not all of the droplets freeze simultaneously, or in a random sequence. There is a freezing front that propagates unidirectionally across the surface. This freezing front may be propagating through a mechanism of freezing that is induced from one droplet to the next by contact of an ice crystal with an adjacent water droplet. Further, while the water condensate is initially uniform on all the blades, the freezing front captures adjacent droplets as it moves, leaving some blades without any ice crystals.

These results show a high level of control of ice nucleation and morphology. First, the ice formation is entirely restricted to the tops of the structure. Second, the results from the two blade system studied indicate that control over ice crystal size and spatial symmetry might be possible with this geometrical templating method. Finally, although AgI does tend to induce faceted crystal growth in general, it is also possible that the geometrical templating of the SHS has an effect on the observed square shape of the ice. It is important to note that we did not observe such consistent ice nucleation behavior in control experiments without the AgI nanoparticles. With no defined nucleation temperature, ice nucleation cannot repeatedly take place at the same stage of water condensation. With AgI at the tips, nucleation predictably occurs at ≈−4 to −5 °C. This was not the case for surfaces with only PVA and colloids at the tips. Precise control over humidity and ice nucleation is required to force water droplets of a specific size and location to freeze before they have a chance to coalesce with adjacent neighbors.

3. Conclusions

By taking advantage of the limited area of contact of a non-wetting solution with a superhydrophobic surface, we were able to locally deposit water- and ice-nucleating materials on the tops of various topographical structures. With this bottom-up approach, we have demonstrated a method to control the condensation and freezing of microscopic droplets on topographical surfaces that is analogous to aspects of how certain natural organisms control condensation and freezing. With the use of (hydrophilic) polyvinyl alcohol at the tips we have achieved a very high level of spatial control over the nucleation, growth, and coalescence of micrometer-scale water droplets. The behavior of water droplets nucleated at the hydrophilic/PVA tips of various patterned geometrical features showed interesting behavior such as extremely uniform nucleation and growth rates and, qualitatively, an increased stability against coalescence. In certain geometrical systems, the water droplets were shown to nucleate from thin-film rupture or to possess unusual asymmetrical geometries. AgI nanoparticles at the tips of superhydrophobic surfaces were shown to reproducibly elevate the freezing temperature of macroscopic droplets. Further, the combination of PVA and AgI at the tips was shown to induce freezing of uniformly condensed water droplets at

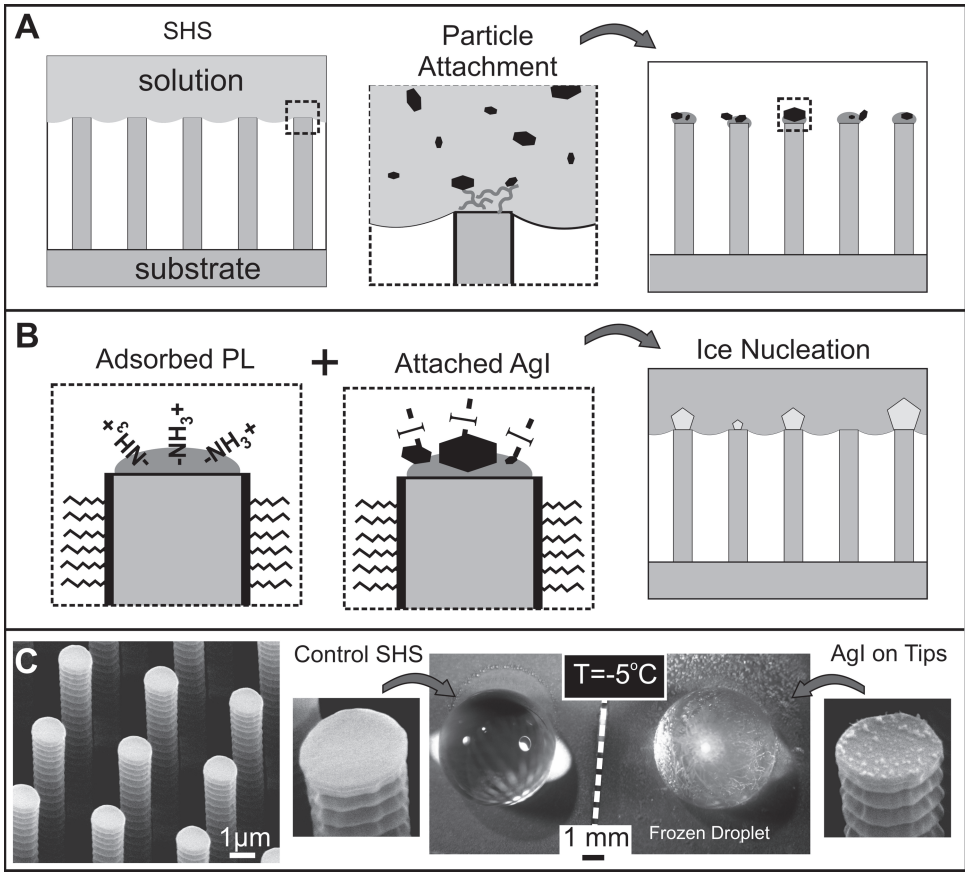

Figure 5. Deposition of ice-nucleating particles on the tips of the posts. A) A schematic shows the general concept of using an adsorbed polymer as a "glue" for attaching nanoparticles to the tips. B) Positively charged poly-L-lysine is first adsorbed to tips and is then used to electrostatically attract negatively charged AgI particles for controlled ice nucleation. C) Macroscopic droplets placed on SHS were used to test the effects of silver iodide on ice nucleation. On a surface cooled to –5 °C with "control" posts without silver iodide (SEM left), a water droplet is able to remain liquid for 5–10 min. On a post surface with AgI tips (SEM right), the droplet freezes almost instantaneously when –5 °C is reached. (The substrates are cooled from 20 to –5 °C at 5 °C/s, at ambient humidity of ≈50%).

the tops of two types of blade structures. These results indicate that control over ice crystal size, shape, spatial symmetry, and position might be achieved with a previously unseen level of uniformity and precision using this geometrical templating method. The reproducibility of this templated water- and ice-nucleating system may allow it to serve as a platform for systematically analyzing condensation and freezing phenomena.

4. Experimental Section

Patterned Superhydrophobic Surfaces: Si (100) wafers were etched with various geometrical patterns by a deep reactive ion etching (DRIE) Bosch process.[29] A hydrophobic surface was generated by oxygen plasma (Diener Electric GmbH Femto-A plasma cleaner) cleaning, followed by overnight exposure of the cleaned samples to (heptadecafluoro-1,1,2,2-tetrahydrodecyl)-trichlorosilane) (Gelest) under vacuum.

Polymer Deposition: A solution of polyvinyl alcohol (PVA) was prepared by mixing 0.25 g of PVA (Fluka 6-98, $M_w \approx 47\,000$) with 100 mL of DI H_2O, and then dissolving the polymer in solution at 60–100 °C while stirring. Poly-L-lysine (0.1% in H_2O, Sigma Aldrich) was used as purchased. For polymer deposition, a droplet (≈3 mm) of the polymer solution was placed on a superhydrophobic surface and then a pipette tip was used to slide the droplet along the surface at a rate of ≈1 mm/s.[15]

Colloid Particle Deposition: 450 nm amidine-terminated (10 vol%) colloidal particles were purchased from Invitrogen and deposited on PVA-coated tips by the same droplet sliding method described in polymer deposition (except with a droplet of colloidal suspension instead of a polymer solution).

AgI Synthesis and Deposition: To synthesize AgI nanoparticles, potassium iodide (KI, 99.99%) and silver nitrate ($AgNO_3$, 99.9999%) were purchased from Sigma-Aldrich. We added 10 μL of a 1 M aqueous KI solution to a 10 mL of rapidly stirring deionized water in a 20-mL borosilicate vial. Then, 5 μL of a 1 M aqueous $AgNO_3$ solution was added to the solution. After addition, the solution immediately turned yellowish-white due to the formation of AgI nanoparticles. (Both aqueous solutions were freshly prepared.) Synthesized AgI nanoparticles varied in diameter between 50 and 150 nm, based on SEM image analysis.

The solution was then deposited onto superhydrophobic surfaces with polymer/colloid-coated tips in the same way as the other aqueous solutions were deposited.

In Situ Condensation Experiments (Optical Microscope Setup): The optical microscope setup is shown in Supporting Information Figure S1. A thermoelectric cooler (Instec TS62) and temperature controller (Instec STC200) were used to cool a sample (silicon SHS) while it was exposed to humid air generated by an ultrasonic humidifier (Holmes Humidifier HM1761). An upright optical microscope (Leica DMRX) and digital color camera (Media Cybernetics/Q-Imaging, Evolution VF-F-CLR-12-C) were used to image the sample. Condensation experiments were carried out

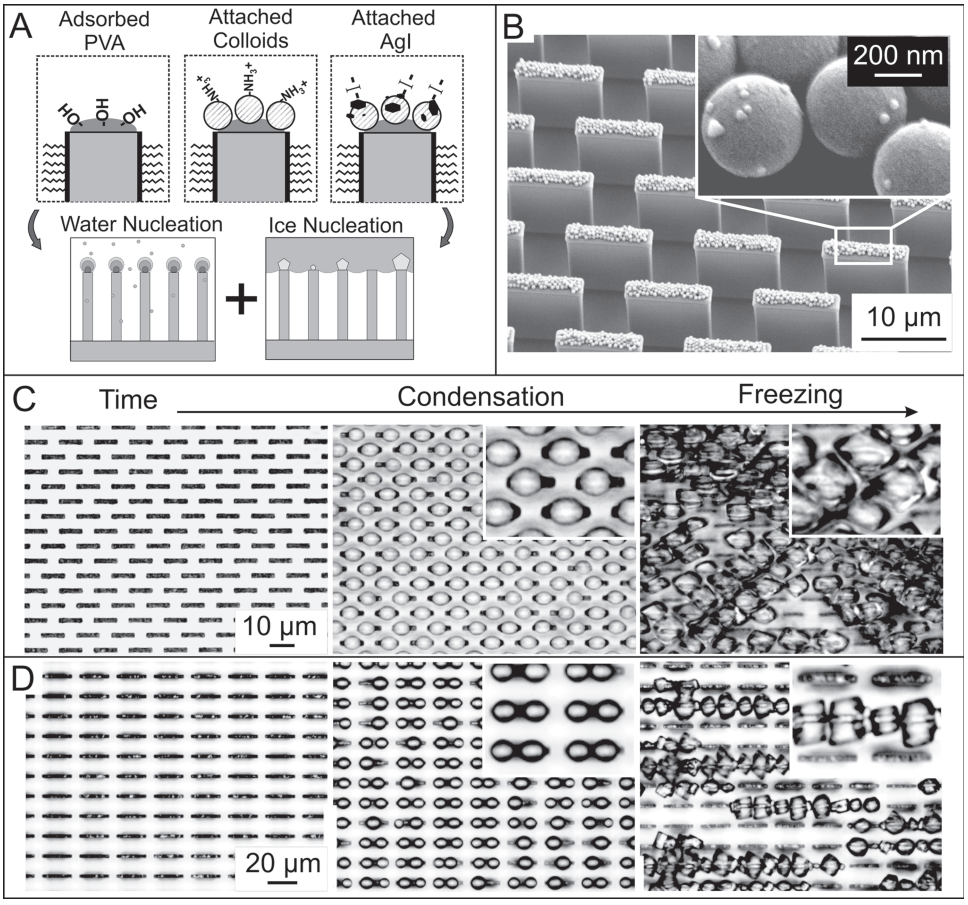

Figure 6. Controlling water condensation and freezing. A) Schematic of the sequential deposition of PVA (–), amidine(+)-terminated colloids, and AgI (–) on the tips of SHS for combined water and ice nucleation experiments. B) An SEM showing a blade SHS with PVA, colloids and attached AgI particles on the tips. C) Condensation and freezing experiments on staggered blades resulted in diagonally arranged, square ice crystals approximately the size of the blades. D) Condensation and freezing on longer, non-staggered blades resulted in linearly arranged, mostly square and rhombus-shaped ice crystals approximately half the length of the blade.

in ≈45% ambient humidity and humid air (65–70% humidity) was blown continuously onto the sample as it was cooled to +5 °C at 0.5 °C/s.

In Situ Ice Experiments: The same setup was used as with condensation (above), except the humidifier was not used. Samples were cooled to –15 °C at 0.5 °C/s under ≈49% ambient humidity.

In Situ Condensation Experiments (Environmental SEM): Samples were placed onto a tilting microscope cooling stage accessory within the Zeiss EVO SEM chamber. The following conditions were used. EHT: 25 kV (backscatter detector); temperature ≈ 1 °C; pressure ≈ 700 Pa. For in situ imaging, we began at a lower chamber pressure (or a higher substrate temperature), above the dew point, and then slowly increased the pressure (or lowered the temperature) until droplet nucleation was observed.

Supporting Information

Supporting Information is available from Wiley Online Library or from the author.

Acknowledgements

The work was partially supported by the ARPA-E under award #: DE-AR0000326. The work was performed in part at the Center for Nanoscale Systems (CNS), a member of the National Nanotechnology Infrastructure Network (NNIN), which is supported by the National Science Foundation under Award ECS-0335765. L.M. thanks the US Department of Homeland Security (DHS) for the fellowship. The DHS Scholarship and Fellowship Program is administered by the Oak Ridge Institute for Science and Education (ORISE) through an interagency agreement between the US Department of Energy (DOE) and DHS. ORISE is managed by Oak Ridge Associated Universities (ORAU) under DOE Contract DE-AC05-06OR23100. Authorship of this manuscript was adjusted September 25, 2013.

Received: February 1, 2013
Revised: June 4, 2013
Published online: July 3, 2013

[1] A. R. Parker, C. R. Lawrence, *Nature* **2001**, *414*, 33–34.
[2] J. Ju, H. Bai, Y. Zheng, T. Zhao, R. Fang, L. Jiang, *Nat. Commun.* **2012**, *3*, 1247.
[3] W. Barthlott, T. Schimmel, S. Wiersch, K. Koch, M. Brede, M. Barczewski, S. Walheim, A. Weis, A. Kaltenmaier, A. Leder, *Adv. Mater.* **2010**, *22*, 2325–2328.
[4] L. R. Maki, E. L. Galyan, M. M. Chang-Chien, D. R. Caldwell, *Appl. Microbiol.* **1974**, *28*, 456–459.

[5] R. Iannone, D. Chernoff, A. Pringle, S. Martin, A. Bertram, *Atmos. Chem. Phys* **2011**, *11*, 1191–1201.
[6] J. G. Duman, *Ann. Rev. Physiol.* **2001**, *63*, 327–357.
[7] G. P. Lopez, H. A. Biebuyck, C. D. Frisbie, G. M. Whitesides, *Science* **1993**, *260*, 647–649.
[8] C. H. Chen, Q. Cai, C. Tsai, C. L. Chen, G. Xiong, Y. Yu, Z. Ren, *Appl. Phys. Lett.* **2007**, *90*, 173108–173110.
[9] K. A. Wier, T. J. McCarthy, *Langmuir* **2006**, *22*, 2433–2436.
[10] C. Dorrer, J. Rühe, *Langmuir* **2007**, *23*, 3820–3824.
[11] R. Narhe, D. Beysens, *Langmuir* **2007**, *23*, 6486–6489.
[12] N. Miljkovic, R. Enright, Y. Nam, K. Lopez, N. Dou, J. Sack, E. N. Wang, *Nano Lett.* **2013**, *13*, 179–187.
[13] K. K. Varanasi, M. Hsu, N. Bhate, W. S. Yang, T. Deng, *Appl. Phys. Lett.* **2009**, *95*.
[14] J. W. Krumpfer, T. J. McCarthy, *J. Am. Chem. Soc.* **2011**, *133*, 5764–5766.
[15] B. D. Hatton, J. Aizenberg, *Nano Lett.* **2012**, *12*, 4551–4557.
[16] M. Kozlov, M. Quarmyne, W. Chen, T. J. McCarthy, *Macromolecules* **2003**, *36*, 6054–6059.
[17] R. Sigsbee, in *Nucleation* (Ed: A. C. Zettlemoyer) Marcel Dekker, New York **1969**, pp. 151–224.
[18] H. Rapaport, I. Kuzmenko, M. Berfeld, K. Kjaer, J. Als-Nielsen, R. Popovitz-Biro, I. Weissbuch, M. Lahav, L. Leiserowitz, *J. Phys. Chem. B* **2000**, *104*, 1399–1428.
[19] D. Turnbull, *J. Chem.Phys.* **1950**, *18*, 198.
[20] C. T. Crowe, *Multiphase Flow Handbook*, CRC, Boca Raton, FL, USA **2005**.
[21] E. Mendizabal, J. Castellanos-Ortega, J. Puig, *Colloids Surf.* **1992**, *63*, 209–217.
[22] J. Glass, *J. Phys. Chem.* **1968**, *72*, 4450–4458.
[23] M. A. Rampi, O. J. A. Schueller, G. M. Whitesides, *Appl. Phys. Lett.* **1998**, *72*, 1781–1783.
[24] G. Edwards, L. Evans, V. La Mer, *J. Colloid Sci.* **1962**, *17*, 749–758.
[25] B. Vonnegut, *J. Appl. Phys.* **1947**, *18*, 593–595.
[26] C. A. Stan, G. F. Schneider, S. S. Shevkoplyas, M. Hashimoto, M. Ibanescu, B. J. Wiley, G. M. Whitesides, *Lab Chip* **2009**, *9*, 2293–2305.
[27] J. W. Goodwin, *Colloids and Interfaces with Surfactants and Polymers: An Introduction*, John Wiley and Sons, Hoboken, NJ, USA **2004**.
[28] G. Edwards, L. Evans, *Trans. Faraday Soc.* **1962**, *58*, 1649–1655.
[29] T. N. Krupenkin, J. A. Taylor, E. N. Wang, P. Kolodner, M. Hodes, T. R. Salamon, *Langmuir* **2007**, *23*, 9128–9133.